Electronic Supplementary Material (ESI) for Journal of Materials Chemistry A.

Supporting Information

Spatially Confined Synthesis of Flexible and Hierarchically Porous Three Dimensional Graphene/FeP Hollow Nanospheres Composite Anode for Highly Efficient and Ultrastable Potassium Ion Storage

Zhifang Zhang,[a] Chenxiao Wu,[a] Zhonghui Chen,[b,*] Huiyu Li,[a] Haijing Cao,[a] Xiaojing Luo,[a] Zebo Fang,[c] and Yanyan Zhu[a,*]

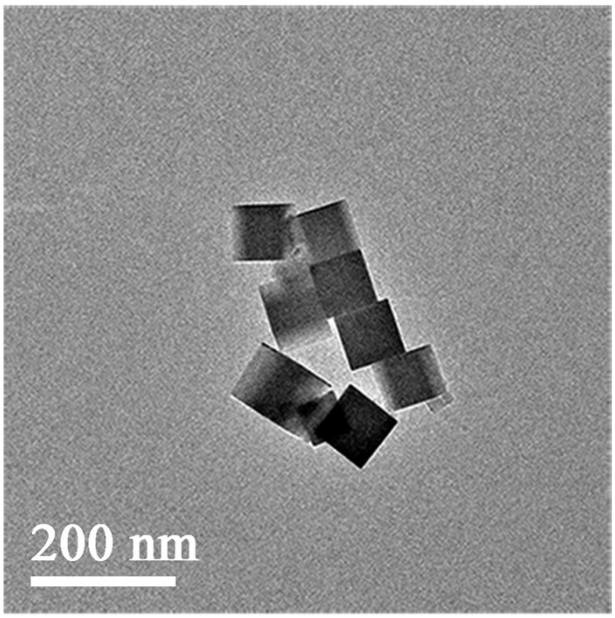

Fig. S1. Pure PB synthesized in the absence of GO under the same procedure as the GO/PB composites.

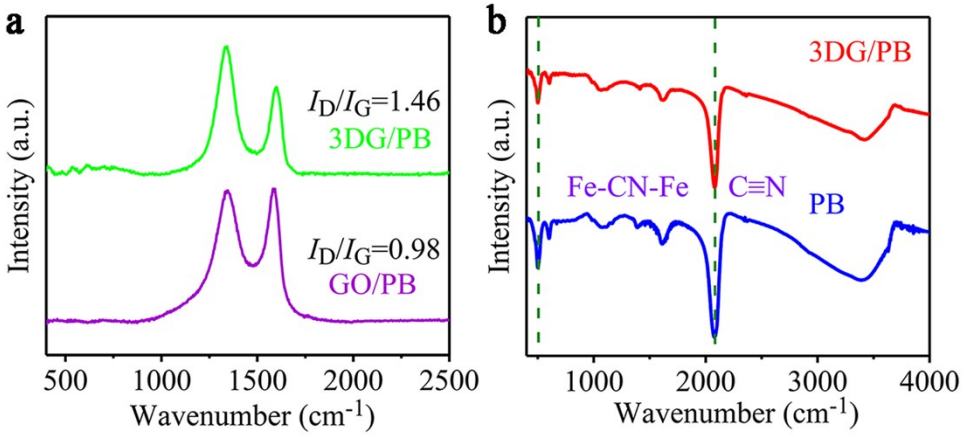

Fig. S2. (a) Raman spectra of GO/PB and 3DG/PB. (b) FTIR spectra of PB and 3DG/PB.

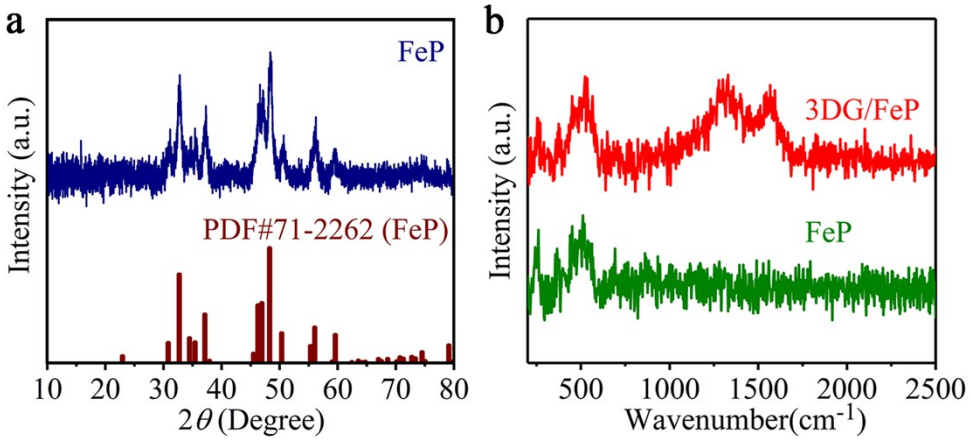

Fig. S3. The XRD pattern of (a) FeP, (b)3DG/FeP and FeP.

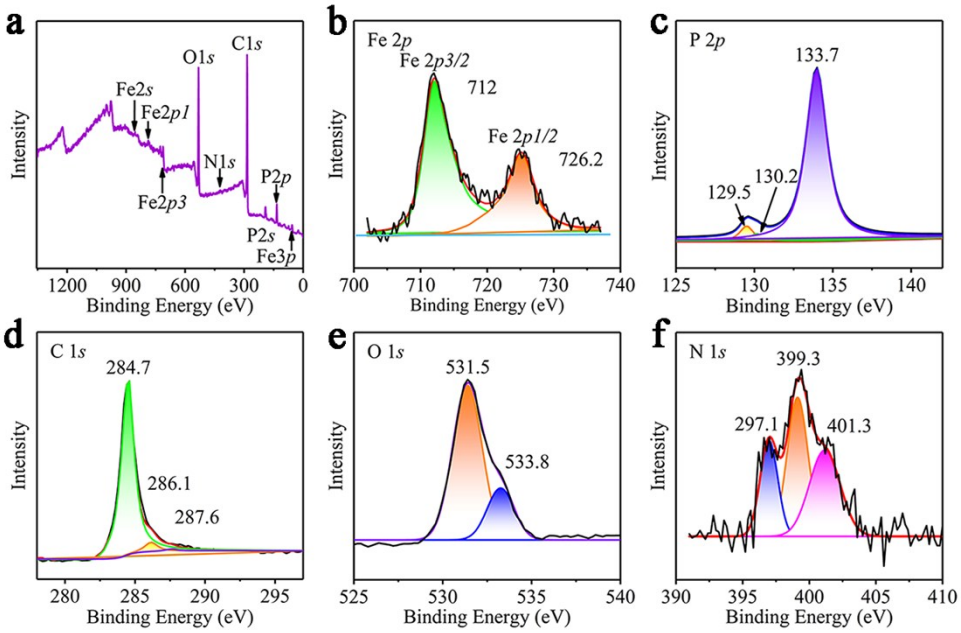

Fig. S4. (a) XPS survey spectrum, (b) Fe 2p, (c) P 2p, (d) C 1s, (e) O 1s and (f) N 1s spectra of the 3DG/FeP.

In the XPS survey spectrum of the 3DG/FeP, the elements of Fe, N, C, P could be detected, which indicated the successful phosphorization of 3DG/PB (Fig. S2a). Peaks at 712 and 726.2 eV corresponds to the Fe 2p, and peaks located at 129.5 and 130.2 eV are assigned to P 2p1/2 and P 2p3/2 of P-Fe respectively (Fig. S2b and c). Furthermore, the P 2p peaks at 133.4 eV can be related to the P=O. The peaks at 284.7, 286.1, and 287.6 eV of C 1s show the existence of C-C (sp2 C), C-N, and C=O bonds, respectively (Fig. S2d and e). The high intensity C-C peak indicates that the GO has been well reduced to rGO. In addition, N signals (397.1, 399.3, and 401.3 eV) are also observed for 3DG/FeP (Figure S2f), which comes from the -C≡N- in PB.

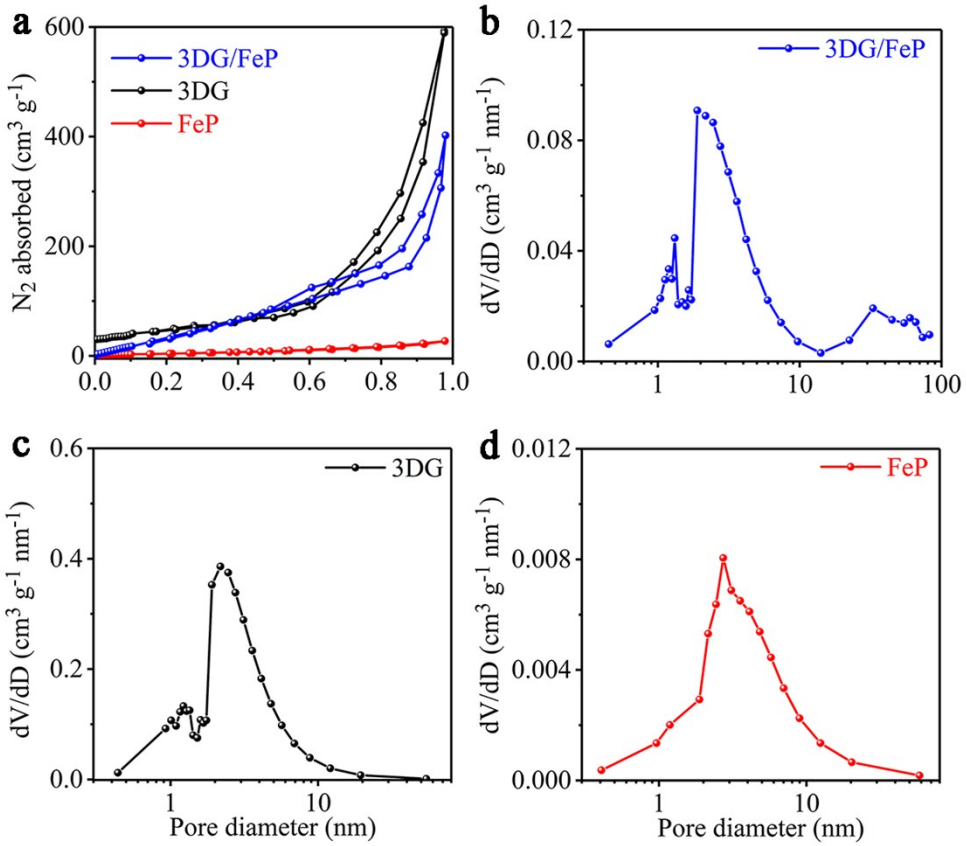

Fig. S5. (a) The N_2 adsorption-desorption isotherms, the pore-size distribution of (b) 3DG/FeP, (c) 3DG, and (d) FeP.

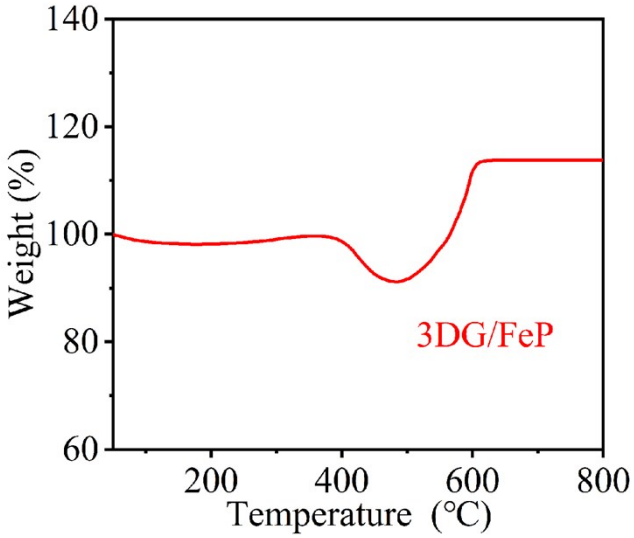

Fig. S6. The TGA curve of 3DG/FeP in air at a heating rate of 10 °C min^{-1}.

FeP content was measured in detail according to the calculation method of the reported carbon-based FeP.[S1] The weight content of FeP in samples were estimated as follows:

$$FeP \rightarrow 1/2\ Fe_2O_3 + 1/2\ P_2O_5$$

$$x \qquad 0.92x \qquad 0.82x$$

Assuming the FeP content is x, the weight fractions for FeP was calculated as the following formula: $0.92\ x + 0.82\ x - (1- x) = 114$ %. Therefore, the FeP content in the 3DG/FeP was about 78 %.

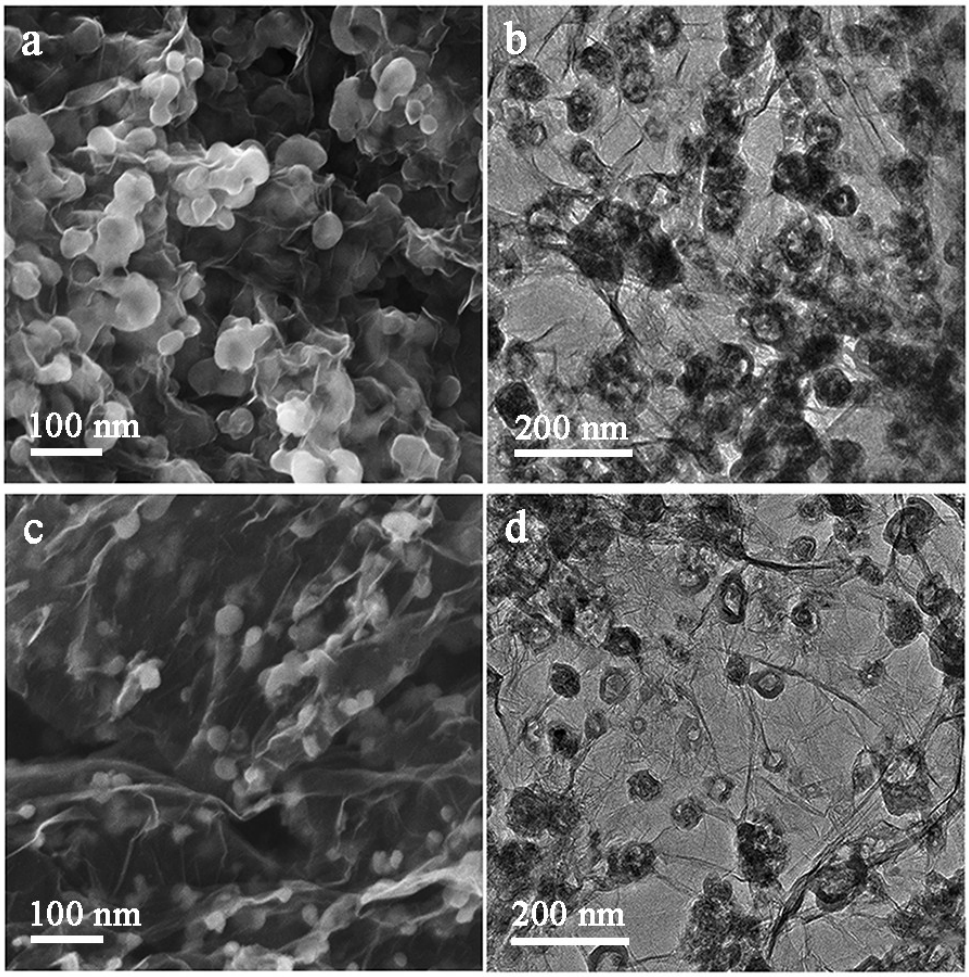

Fig. S7. SEM images of 3DG/FeP-H (a), 3DG/FeP-L (c). TEM images of 3DG/FeP-H (b), 3DG/FeP-L (d) (about 84% of FeP in 3DG/FeP-H and 68% of FeP in 3DG/FeP-L)

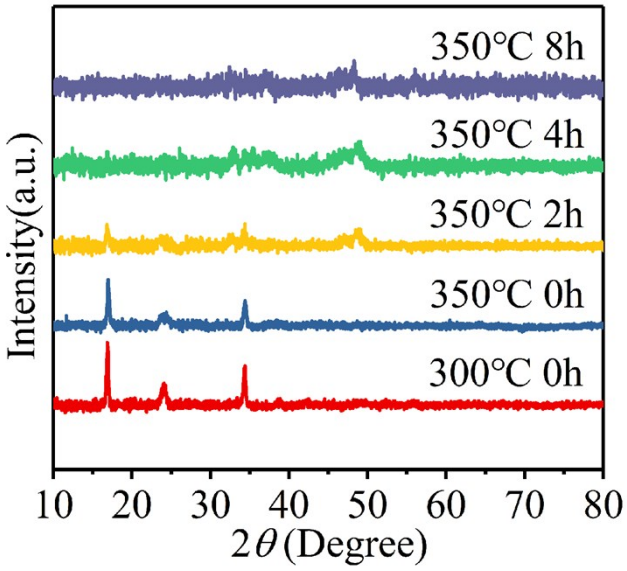

Fig. S8. XRD patterns of the obtained products collected at different reaction temperature for different reaction time, (a) 300 °C 0 h, (b) 350 °C 0 h, (c) 350 °C 2 h, (d) 350 °C 4 h, (e) 350 °C 8 h.

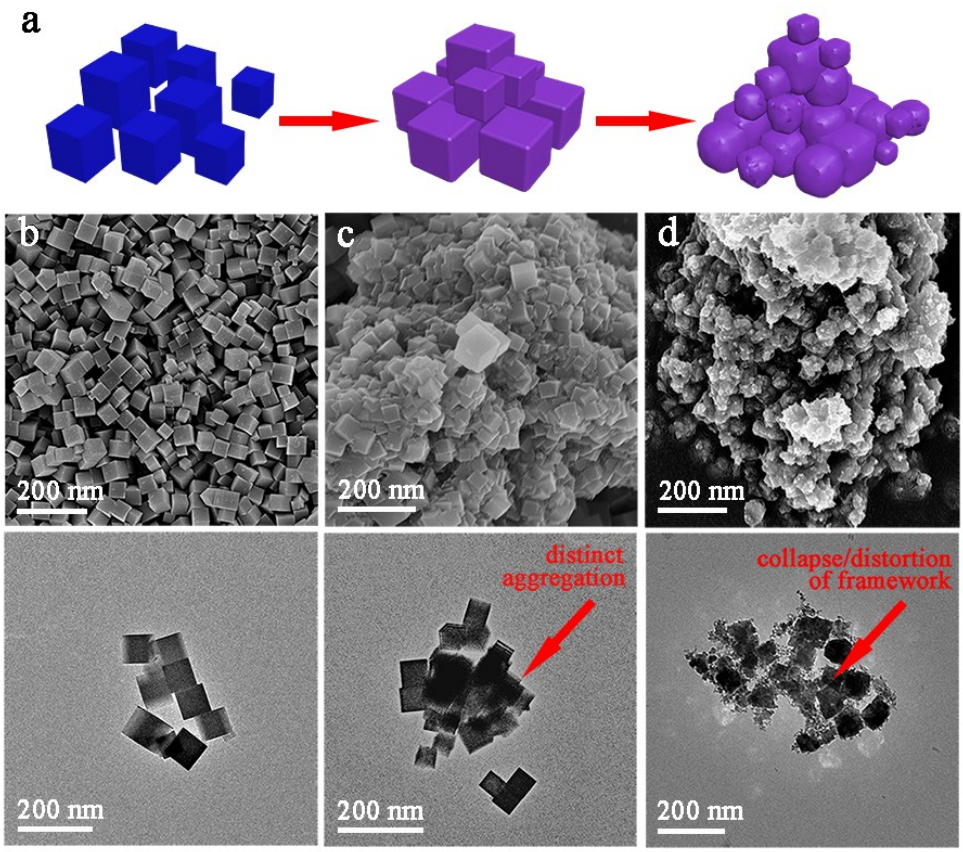

Fig. S9. (a) Thermal conversion diagram of PB. The SEM and TEM images of pure PB (b), FeP after 2 h (c) and 8h (d) thermal doping treatment.

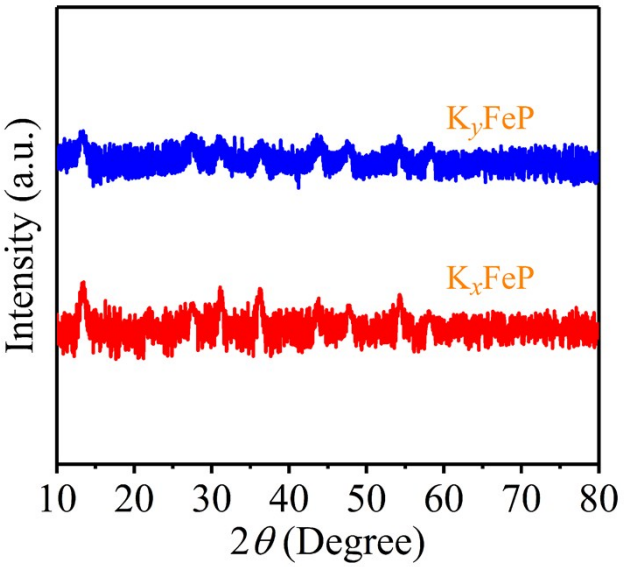

Fig. S10. XRD patterns of the K_xFeP (0.9 V) and K_yFeP (0.6 V) during the first discharge process.

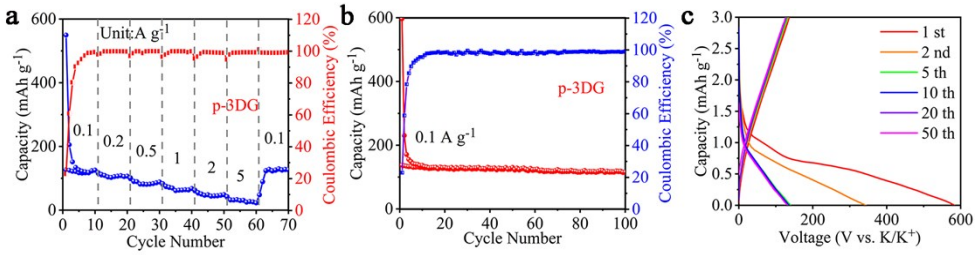

Fig. S11. (a) The rate performance (b) cycling performance of p-3DG anode at 0.1 A g^{-1} for 100 cycles. (c) The charge/discharge curves of p-3DG at 0.1 A g^{-1}.

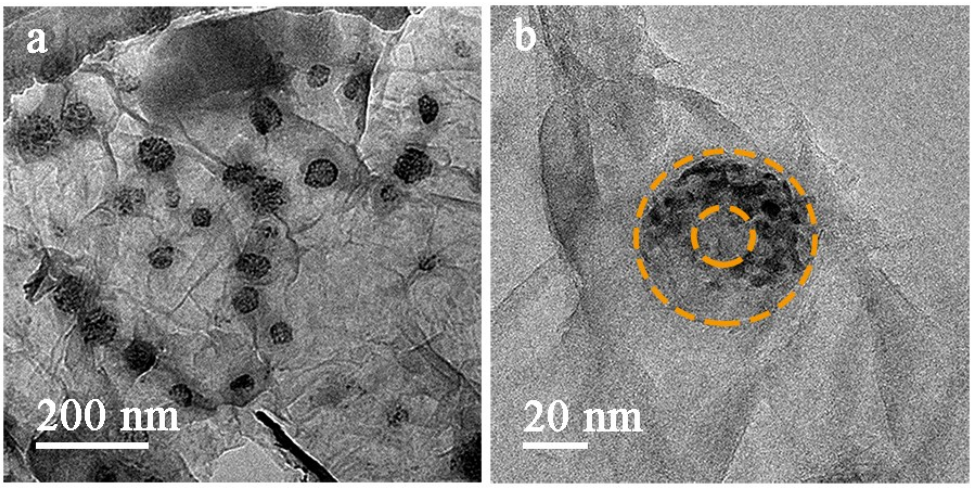

Fig. S12. The TEM images of 3DG/FeP anode after 200 cycles.

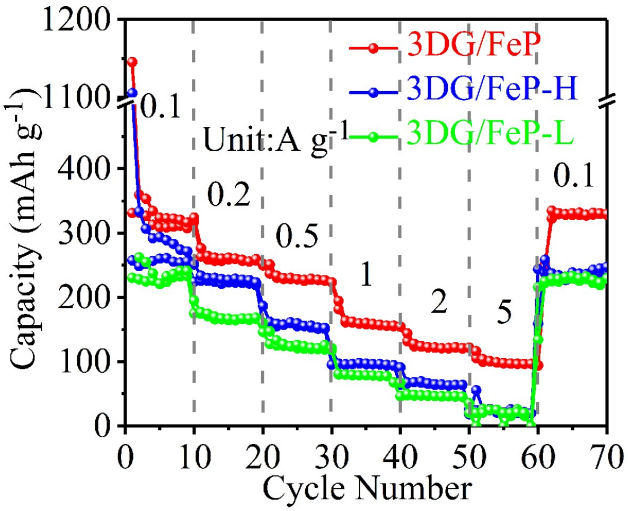

Fig. S13. The rate performance of 3DG/FeP with different mass content of FeP.

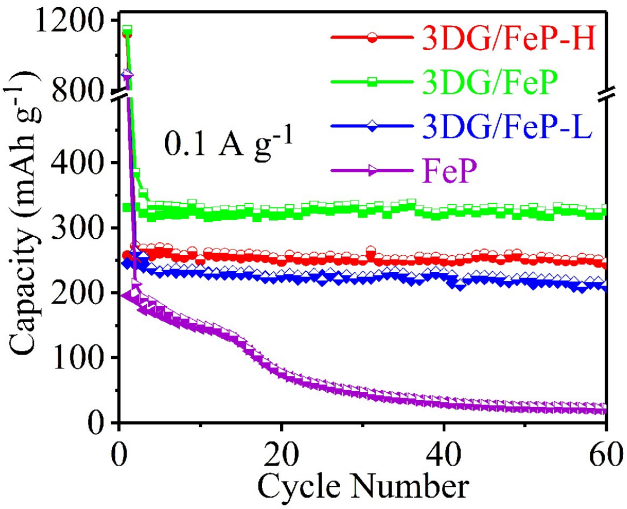

Fig. S14. The cycling performance of 3DG/FeP with different mass content of FeP and pure FeP at 0.1 A g^{-1}.

Table S1. Comparison of recently reported typical FeP-based anode materials for potassium ion batteries.

Materials	Ratio of Active Material	Current Density /mA g^{-1}	Capacity /mAh g^{-1}	Capacity (By Electrode) /mAh g^{-1}	Cycle Life /Capacity Retention @Cycle Number@mA g^{-1}	Ref
CoP/C	80%	50	126.72	101.4	~75%@200@200 mA g^{-1}	S2
		1000	54.4	43.52		
FeP@C	80%	100	220	176	92%@300@100 mA g^{-1}	S3
		2000	40	32		
ZnS@C@rGO	90%	50	320	297	~25%@300@500 mA g^{-1}	S4
		500	240	187.2		
MoS_2/rGO	80%	100	380	304	100@100 mAg^{-1}	S5
$MoSe_2$/N-C	80%	100	258	206.4	88%@200@100 mA g^{-1}	S6
Sn/C	80%	25	150	120	75%@30@25 mA g^{-1}	S7
$FeCl_3$-EG	80%	50	269.5	215.6	88.82%@500@100 mA g^{-1} 70%@1300@5000 mA g^{-1}	S8
VS_2/NSA	60%	1000	175.4	105.24	105%@100@1000 mA g^{-1}	S9
		5000	133.1	79.86		
$K_2Ti_8O_{17}$	70%	100	400	280	85%@50@20 mA g^{-1}	S10
		2000	100	70		
Hybrid Co_3O_4-Fe_2O_3/C	66.6%	20	120	79.92	93%@180@50 mA g^{-1}	S11
		500	50	33.3		
Ordered Mesoporous Carbon	80%	50	257.4	205.92	99%@20@50 mA g^{-1}	S12
		1000	146.5	117.2		
Soft Carbon	70%	500	200	140	71.4%@1000@350 mA g^{-1}	S13
Oak-based Hard Carbon	80%	100	135	108	98%@150@100 mA g^{-1}	S14
Semi-hollow Microro Soft Carbon	70%	100	312	218.4	82%@500@200 mA g^{-1}	S15
		500	180	126		

Hard-soft Composite Carbon	80%	100	261	208.8	93%@450@200 mA g^{-1}	S16
		10000	120	96		
Graphitic Carbon Networks	80%	100	220	176	75%@500@50 mA g^{-1}	S17
		2000	100	80		
Graphite	90%	20	246	221.4	98%@200@20 mA g^{-1}	S18
		500	~0	~0		
Reduced Graphene Oxide	80%	5	280/205	224	100%@175@10 mA g^{-1}	S19
		100	50	40		
FFGF (F-Doped Graphene Foam)	70%	50	326.1	228.27	90.91%@50@60 mA g^{-1}	S20
		500	165.9	116.13	88.24%@500@500 mA g^{-1}	
N-doped Graphene	100%	50	350	350	77.78%@100@100 mA g^{-1}	S21
This Work	100%	100	323	323	97.3%@300@100 mA g^{-1}	
		2000	127	127	97.6%@2000@2000 mA g^{-1}	

References

S1 Q. Wang, B. Wang, Z. Zhang, Y. Zhang, J. Peng, Y. Zhang and H. Wu, *Inorg. Chem. Front.,* 2018, **5**, 2605-2614.
S2 J.Bai, B. Xi, H. Mao, Y. Lin, X. Ma, J. Feng and S. Xiong, *Adv. Mater.,* 2018, **30**, 1802310-1802317.
S3 F. Yang, H. Gao, J. Hao, S. Zhang, P. Li, Y. Liu, J. Chen and Z. Guo, *Adv. Funct. Mater.,* 2019, **29**, 1808291-1808298.
S4 J. Chu, W. Wang, J. Feng, C.-Y. Lao, K. Xi, L. Xing, K. Han, Q. Li, L. Song and P. Li, *ACS Nano,* 2019, **13**, 6906-6916.
S5 K. Xie, K. Yuan, X. Li, W. Lu, C. Shen, C. Liang, R. Vajtai, P. Ajayan and B. Wei, *Small,* 2017, **13**, 1701471-1701479.
S6 J. Ge, L. Fan, J. Wang, Q. Zhang, Z. Liu, E. Zhang, Q. Liu, X. Yu, and B. Lu, *Adv. Energy Mater.,* **2018**, *8*, 1801477-1801484.
S7 I. Sultana, T. Ramireddy, M. M. Rahman, Y. Chen and A. M. Glushenkov, *Chem. Commun.,* 2016, **52**, 9279-9282.
S8 D. Li, M. Zhu, L. Chen, L. Chen, W. Zhai, Q Ai, G. Hou, Q. Sun, Y. Liu, and Z. Liang, *Adv. Mater. Inter.,* 2018, **5**, 1800606-1800615.
S9 J. Zhou, L. Wang, M. Yang, J. Wu, F. Chen, W. Huang, N. Han, H. Ye, F. Zhao and Y. Li, *Adv. Mater.,* 2017, **29**, 1702061-1702069.
S10 J. Han, M. Xu, Y. Niu, G.-N. Li, M. Wang, Y. Zhang, M. Jia, C. M. Li, *Chem. Commun.,* 2016, **52**, 11274-11276.
S11 I. Sultana, M. M. Rahman, S. Mateti, V. G. Ahmadabadi, A. M. Glushenkov and Y. Chen, *Nanoscale,* 2017, **9**, 3646-3654.
S12 W. Wang, J. Zhou, Z. Wang, L. Zhao, P. Li, Y. Yang, C. Yang, *Adv. Energy Mater.,* 2018, **8**, 1701648-1701656.
S13 L. Fan, K. Lin, J. Wang, R. Ma, B. Lu, *Adv. Mater.,* 2018, **30**, 1800804-1800811.
S14 S. R. Prabakar, S. C. Han, C. Park, I. A. Bhairuba, M. J. Reece, K.-S. Sohn and M. Pyo, *J. Electrochem. Soc.,* 2017, **164**, A2012-A2016.
S15 X.Wang, K. Han, D. Qin, Q. Li, C. Wang, C. Niu, L. Mai, *Nanoscale,* 2017, **9**, 18216-18222.
S16 Z. Jian, S. Hwang, Z. Li, A. S. Hernandez, X. Wang, Z. Xing, D. Su, and X. Ji, *Adv. Funct. Mater.,* 2017, **27**, 1700324-1700330.
S17 W. Zhang, X. Jiang, X. Wang, Y. V. Kaneti, Y. Chen, J. Liu, J. S. Jiang, Y. Yamauchi and M. Hu, *Angew. Chem. Int. Ed.,*

2017, **56**, 8435-8440.
S18 J. Zhao, X. Zou, Y. Zhu, Y. Xu and C. Wang, *Adv. Funct. Mater.,* 2016, **26**, 8103-8110.
S19 W. Luo, J. Wan, B. Ozdemir, W. Bao, Y. Chen, J. Dai, H. Lin, Y. Xu, F. Gu and V. Barone, *Nano Lett.,* 2015, **15**, 7671-7677.
S20 Z. Ju, S. Zhang, Z. Xing, Q. Zhuang, Y. Qiang and Y. Qian, *ACS Appl. Mater. Inter.,* 2016, **8**, 20682-20690.
S21 K. Share, A. P. Cohn, R. Carter, B. Rogers, C. L. Pint, *ACS Nano,* 2016, **10**, 9738-9744.